Microphysical Timescales in Clouds and their Application in Cloud-Resolving Modeling

Xiping Zeng*

Goddard Earth Sciences and Technology Center, University of Maryland, Baltimore County, and Laboratory for Atmospheres, NASA Goddard Space Flight Center, Greenbelt, Maryland

Wei-Kuo Tao and Joanne Simpson

Laboratory for Atmospheres, NASA Goddard Space Flight Center, Greenbelt, Maryland

October 6, 2004

To be submitted to *Journal of the Atmospheric Sciences*

Corresponding author address: Dr. Xiping Zeng, Mail Code 912, Rm A417, Bldg 33, NASA/Goddard Space Flight Center, Greenbelt, MD 20771. Email: zeng@agnes.gsfc.nasa.gov

Abstract

Computational phenomena (i.e., spurious supersaturation and negative mixing ratio of cloud water) usually exist in cloud-resolving models when the time step for explicit integration is larger than a microphysical timescale in clouds. In this paper, the microphysical timescales in clouds are studied, showing that the timescale of water vapor condensation (or cloud water evaporation) is smaller than 10 s — the order of a typical time step for cloud-resolving models. To avoid spurious computational phenomena in cloud-resolving modeling, it is suggested that moist entropy be used as a prognostic thermodynamic variable, and temperature be diagnosed from that and other prognostic variables. A simple numerical model with moist entropy as a prognostic variable, for example, is presented to show that spurious computational phenomena are removed when moist entropy is used as a prognostic variable.

1. Introduction

With the continuous increase in computational power, cloud-resolving models will be used in the near future to simulate explicitly clouds and large-scale circulations for their interaction. For the correct simulation of that interaction, the models should well represent not only the processes in relation to the life cycle of individual clouds systems but also the processes in relation to large-scale circulations.

In the Tropics, deep cumulus clouds act as an engine for the atmosphere, driving large-scale vertical circulations through convective heating (Riehl and Malkus 1958). However, many questions on convective heating need to be addressed through observations and modeling (e.g., Simpson *et al.* 1988, Tao and Adler 2003a). One of the questions is on the "efficiency" of the engine. Since clouds consist of small particles, the "efficiency" is related to the microphysics in clouds. Hence the microphysics should be represented properly in a cloud-resolving model in order to accurately simulate the interaction between clouds and large-scale circulations.

On the other hand, small particles in clouds absorb and emit radiation, which can change the atmospheric energy budget and in turn large-scale circulations. As a result, they are coupled with large-scale circulations (e.g., Raymond 2000, Raymond and Zeng 2000). Since large-scale vertical circulations are sensitive to the atmospheric radiative cooling rate (e.g., Zeng *et al.* 2004) and the radiative cooling rate is modulated by clouds through cloud microphysics (e.g., Albrecht and Cox 1975; Baker 1997), cloud microphysics must be represented properly in a cloud-resolving model for the accurate

simulation of radiation and its role in the interaction between clouds and large-scale circulations.

In current cloud-resolving models, there are computational phenomena such as spurious supersaturation near cloud edges (e.g., Grabowski 1989), and special adjustment techniques are usually introduced to reduce their negative effects, benefiting the numerical simulation of individual cloud systems (e.g., Tao *et al.* 1989). Some computational phenomena originate in the choice of prognostic thermodynamic variables (Grabowski 1989; Ooyama 1990; Zeng 2001; Zeng, Tao and Simpson 2004). In a new trend to avoid them, moist entropy is used as a prognostic variable in modeling, and temperature is diagnosed from that and other prognostic variables (Raymond and Blyth 1986; Ooyama 1990, 2001; Zeng 2001, Zeng, Tao and Simpson 2004). Raymond and Blyth (1986) used moist entropy and the total mixing ratio of airborne water (water vapor and cloud water) as prognostic variables in a parcel model. Ooyama (1990) analyzed the thermal relations of moist entropy and suggested moist entropy be used as a prognostic variable in multi-dimensional numerical models. Ooyama (2001) and Zeng (2001) constructed two- and three-dimensional models with moist entropy as a prognostic variable, respectively, to simulate warm clouds. In their models, neither spurious supersaturation nor negative mixing ratio of cloud water appears. Thus it is logical to extend moist entropy as a prognostic variable to simulate cold clouds. Zeng, Tao and Simpson (2004) derived a precise equation for moist entropy, providing a theoretical basis for moist entropy to be used as a prognostic variable in the modeling of cold clouds. In this paper, another aspect of moist entropy is addressed: the benefit of using moist entropy as a prognostic variable.

Spurious computational phenomena, as shown in section 2, exist in a numerical model when the time step for explicit integration is larger than a physical timescale. The phenomena manifest themselves in cloud-resolving modeling as spurious supersaturation and negative mixing ratio of cloud water. Since the proper simulation of the mixing ratio of cloud water is vital in long-term cloud-resolving modeling (e.g., Robe and Emanuel 1996), the origin of computational phenomena should be explored so that they can be removed. Thus, the microphysical timescales in clouds should be studied first in contrast to the time step for cloud-resolving modeling.

The microphysical timescale of water vapor condensation (or cloud water evaporation), as shown in section 3, is smaller than 10 s — the order of a typical time step for cloud-resolving models. Thus, the small timescale can bring about computational phenomena in cloud-resolving modeling. To avoid spurious phenomena, it is suggested in section 4 that moist entropy be used as a prognostic variable in the place of temperature. That strategy is different from other technologies on cloud condensation modeling (e.g., Grabowski 1989; Tao *et al.* 1989; Grabowski and Smolarkiewicz 1990; Margolin, Reisner and Smolarkiewicz 1997).

This paper is composed of five sections. In section 2, a spurious computational phenomenon is illustrated with the aid of a simple numerical model. In section 3, the expressions for microphysical timescales in clouds are derived, and the timescales are compared with the time steps used in cloud-resolving modeling. In section 4, the choice of prognostic thermodynamic variables in cloud-resolving modeling is discussed, and a numerical model with moist entropy as a prognostic variable is presented, as an example, to show that computational phenomena are removed when moist entropy is used as a

prognostic variable. In section 5, a summary is given. Except for special illustrations, the paper follows the symbol definitions in Appendix A.

2. Spurious computational phenomena

In this section, an example of spurious computational phenomena is illustrated with a simple numerical model whose corresponding differential equation is

$$d\phi/dt = -\phi/\tau, \tag{2.1}$$

where the variable ϕ is a function of time t and the constant τ is a timescale. The variable ϕ=1 when t=0. Equation (2.1) is solved analytically with $\phi = \exp(-t/\tau)$.

For explicit integration, Equation (2.1) is discretized as

$$\phi^{n+1} = \phi^n - \phi^n \Delta t/\tau \tag{2.2}$$

where superscripts indicate time level and Δt is the time step for integration. Equation (2.2) is solved with $\phi^n = (1-\Delta t/\tau)^n$. Obviously the numerical solution of Equation (2.2) is close to the analytical solution of Equation (2.1) when

$$\Delta t < \tau. \tag{2.3}$$

Otherwise, the value of ϕ^n blows up or oscillates spuriously around zero.

The computational phenomenon when $\Delta t > \tau$ is shown in Figure 1, where Δt=10 s and the timescale τ is 2, 5 and 12.5 s, respectively. The numerical solutions of Equation (2.2) and their corresponding analytical solutions are shown with thick and thin lines, respectively, in the same pane for comparison. The values for ϕ blows up when τ=2 s (or $\Delta t > 2\tau$). When $\Delta t = 2\tau = 10$ s, ϕ oscillates between –1 and 1 spuriously. When τ=12.5 s (or $\Delta t < \tau$), the numerical solution is close to the analytical solution.

Many microphysical processes in clouds are governed by Equation (2.1) or similar equations with different timescales (see section 3 for details). When a microphysical timescale is so small that the condition (2.3) is violated, spurious behavior appears. In the next section, microphysical timescales in clouds are studied so as to provide theoretical evidences for the construction of cloud-resolving models.

3. Microphysical timescales in clouds

a. Condensation growth

An air parcel with uniform cloud droplets is studied for the timescale of water vapor condensation. Only water vapor condensation on cloud droplets or the evaporation of cloud droplets exists in the parcel. The concentration and the radius of droplets in the parcel are denoted with N_c and r_c, respectively, and the mixing ratio of cloud water with q_c. Thus

$$q_c = \frac{4}{3}\pi\rho_w \frac{N_c}{\rho} r_c^3 . \tag{3.1}$$

The growth rate of a droplet due to water vapor condensation is expressed as (e.g., Pruppacher and Klett 1997)

$$\frac{dr_c}{dt} = \frac{A_w(q_v/q_{vsw} - 1)}{r_c}, \tag{3.2}$$

where q_v is the mixing ratio of water vapor, q_{vsw} the saturation mixing ratio of water vapor over water and

$$A_w = (\rho_w L_v^2 / K_a R_v T^2 + \rho_w R_v T / E_{sw} D_v)^{-1} . \tag{3.3}$$

Differentiating Equation (3.1) with respect to time, and then substituting Equation (3.2) into the resulting equation yields

$$\frac{dq_v}{dt} = -\frac{dq_c}{dt} = -4\pi\rho_w A_w r_c \frac{N_c}{\rho}\left(\frac{q_v}{q_{vsw}} - 1\right). \tag{3.4}$$

Assume that the parcel is adiabatic and stationary. Thus, the energy equation is written approximately as

$$C_p \frac{dT}{dt} = -L_v \frac{dq_v}{dt}. \tag{3.5}$$

Substituting Equation (3.4) into (3.5) yields

$$\frac{d(q_v - q_{vsw})}{dt} = -4\pi\rho_w A_w r_c \frac{N_c}{\rho}\left(1 + \frac{q_{vs} L_v^2}{R_v C_p T^2}\right)\frac{q_v - q_{vsw}}{q_{vsw}} \tag{3.6}$$

with the aid of the Clausius-Clapeyron equation

$$\frac{d \ln E_{sw}}{dT} = \frac{L_v}{R_v T^2}. \tag{3.7}$$

The analogy between Equations (3.6) and (2.1) shows the timescale of water vapor condensation

$$\tau = \left(1 + \frac{q_{vsw} L_v^2}{R_v C_p T^2}\right)^{-1} \frac{\rho q_{vsw}}{4\pi\rho_w A_w N_c r_c} \tag{3.8}$$

which is consistent with that of Squires (1952) and Korolev and Mazin (2003).

Equation (3.8) shows that the timescale is a function of temperature and pressure. An ideal case is discussed here to show the variation of the timescale with height. Assume that cloudy air has the same temperature and pressure as its ambient air. The ambient air is stationary. Its surface pressure is 1013.25 hpa, and temperature decreases linearly with height from 288 at z=0 to 216.5 K at z=11 km. For this case, the timescale of water vapor condensation against height is computed with Equation (3.8), and the results for $N_c r_c$=500 and 3000 $\mu m \cdot cm^{-3}$ are displayed in Figure 2 with thin and thick lines, respectively. If r_c=10 μm, $N_c r_c$=500 and 3000 $\mu m \cdot cm^{-3}$ are representative of marine and continental air,

respectively (e.g., Pruppacher and Klett 1997). Both timescales for $N_c r_c$=500 and 3000 μm·cm^{-3}, as shown in the figure, are smaller than 10 s, implying that water vapor condensation on to cloud droplets (or the evaporation of cloud droplets) is not suitable for explicit simulation in cloud-resolving modeling.

b. Other diffusion growth

Similar to the derivation for Equation (3.8), the timescale of water vapor deposition on small ice particles is obtained as

$$\tau = (1 + \frac{q_{vsi} L_s^2}{R_v C_p T^2})^{-1} \frac{\rho q_{vsi}}{4\pi \rho_i A_i N_i r_i}, \tag{3.9}$$

where q_{vsi} is the saturation mixing ratio of water vapor over ice, r_i the radius of small ice particles, N_i the concentration of the ice particles and

$$A_i = (\rho_i L_s^2 / K_a R_v T^2 + \rho_i R_v T / E_{si} D_v)^{-1}. \tag{3.10}$$

Following the procedure in Figure 2, the timescale for vapor deposition is computed with Equation (3.9), and the results for $N_i r_i$=10^{-3}, 10^{-1} and 10^{1} μm·cm^{-3} are displayed in Figure 3. If r_i=10 μm, $N_i r_i$=10^{-3}, 10^{-1} and 10^{1} μm·cm^{-3} represent the air with low, moderate and high concentrations of ice particles, respectively (e.g., Pruppacher and Klett 1997). As shown in the figure, the timescale decreases with the increase of N_i for a given r_i. However, even when the concentration of ice particles is high (or N_i=1000 liter^{-1}), the timescale is still larger than 10 s, implying that water vapor deposition to small ice particles is suitable for explicit simulation in cloud-resolving modeling.

The timescale of rainwater evaporation can be obtained in steps analogous to Equation (3.8). Introducing the ventilation coefficients f_v for water vapor diffusion and f_h for heat

transport in Equation (3.2) for raindrop evaporation and assuming $f_v=f_h$ (e.g., Pruppacher and Klett 1997), the time scale of rainwater evaporation is obtained

$$\tau = (1+\frac{q_{vsw}L_v^2}{R_v C_p T^2})^{-1} \frac{\rho q_{vsw}}{4\pi\rho_w A_w f_v N_r r_r}, \tag{3.11}$$

where N_r and r_r are the concentration and the radius of rain drops, respectively. Let $r_r=10^3$ μm, $N_r=10^3$ m^{-3}, $f_v=10$, $T=280$ K and $p=850$ hpa. The timescale of rainwater evaporation is 323 s. Since the timescale is much larger than 10 s, the order of time step in cloud-resolving modeling, rainwater evaporation is suitable for explicit simulation in cloud-resolving modeling.

Similarly, the time scale of water vapor deposition on precipitating ice particles is obtained after introducing the ventilation coefficients f_v for water vapor diffusion and f_h for heat transport in Equation (3.9). That is

$$\tau = (1+\frac{q_{vsi}L_s^2}{R_v C_p T^2})^{-1} \frac{\rho q_{vsi}}{4\pi\rho_i A_i f_v N_p r_p} \tag{3.12}$$

where N_p and r_p are the concentration and the radius of precipitating ice particles, respectively. Let $r_p=10^3$ μm, $N_p=10^3$ m^{-3}, $T=260$ K and $p=550$ hpa. The timescale of water vapor deposition on snowflakes is 1184 s when $f_v=2$, and the timescale of deposition on graupel is 236 s when $f_v=10$. Since both timescales are much larger than 10 s, water vapor deposition on to snowflakes and graupel is suitable for explicit simulation in cloud-resolving modeling.

c. Ice fusion

An air parcel with uniform spherical ice particles is studied for the timescale of cloud ice fusion. For simplicity, it is assumed that no liquid water surrounds ice particles. Let N_i

and r_i denote the concentration and the radius of ice particles, respectively. The melting of an ice particle is described with (e.g., Pruppacher and Klett 1997).

$$-4\pi\rho_i L_f r_i^2 \frac{dr_i}{dt} = 4\pi r_i f_h K_a (T - T_o) + 4\pi r_i f_v L_v \left(\frac{e}{R_v T} - \frac{E_{sw}(T_o)}{R_v T_o}\right), \tag{3.13}$$

where T_o=273.15 K and e is the partial pressure of water vapor in the air. In the preceding equation, the term on the left side represents the latent cooling due to ice fusion, and the two terms on the right side represent the sensible and latent heat fluxes from air to the ice particle, respectively. Obviously the latent heat of water vapor condensation at the surface is balanced by part of the latent heat of ice melting, and the latent heats do not change air temperature directly.

Assume that the parcel is adiabatic and stationary. For ice fusion, heat is transfered from air to ice particles. Thus air temperature is decreased, which is described as

$$C_p \frac{dT}{dt} = -4\pi r_i f_h K_a \frac{N_i}{\rho}(T - T_o). \tag{3.14}$$

The contrast between Equations (3.14) and (2.1) shows the timescale of ice fusion

$$\tau = \frac{\rho C_p}{4\pi f_h K_a N_i r_i}. \tag{3.15}$$

Using the above expression, the timescales of ice fusion and snowflake fusion are estimated with f_h=1 and 2, respectively. Their results are displayed in Figure 4 with thin and thick lines, respectively.

Equation (3.15) and Figure 4 are also suitable for the freezing of water that is collected by ice particles. As shown in Figure 4, the timescales in relation to fusion and freezing are larger than 10 s. Therefore, the fusion and freezing processes are suitable for explicit simulation in cloud-resolving modeling.

4. Moist entropy as a prognostic variable

The microphysical timescales analyzed in the preceding section show that only the timescale of water vapor condensation is smaller than the typical time step used in cloud-resolving modeling. Since this short timescale may bring about computational phenomena in cloud-resolving modeling, the choice of prognostic thermodynamic variables is discussed in this section for the removal of the computational phenomena.

a. Prognostic thermodynamic variables

To remove the computational phenomenon in Equation (2.2) when $\Delta t > \tau$, it is assumed that ϕ=0 in one step. As shown in Figure 1, ϕ=0 approximates the analytical solution well when $\Delta t > \tau$. In other words, the prognostic variable ϕ degenerates into a diagnostic variable. Next, prognostic thermodynamic variables are discussed for cloud-resolving modeling.

In current cloud-resolving models, three prognostic thermodynamic variables are used to simulate non-precipitating warm clouds and those three variables plus others to simulate other clouds (e.g., Grabowski 1989, Tao and Simpson 1993, Tompkins and Craig 1998, Tao *et al.* 2003b). The three prognostic variables are T temperature (or its equivalent), q_v the mixing ratio of water vapor and q_c the mixing ratio of cloud water. However the three prognostic variables, as shown in Equations (3.4) and (3.5), involve one timescale that is smaller than 10 s the order of time steps used in cloud-resolving modeling. Since *only* one short timescale is involved, it is impossible for all three prognostic variables to degenerate into diagnostic variables at the same time. Thus, it is

suggested that other prognostic variables (e.g., moist entropy) be used for cloud-resolving modeling.

Moist entropy per unit mass of dry air is expressed as (Zeng, Tao and Simpson 2004)

$$s = (C_p + c_l q_t)\ln\frac{T}{T_{ref}} - R_d \ln\frac{p-e}{p_{ref}} + \frac{L_v}{T}q_v - R_v q_v \ln f - \frac{L_f}{T}q_i, \qquad (4.1)$$

where relative humidity $f=e/E_{sw}$; T_{ref} = 273.15 K and p_{ref} = 10^5 pa are the reference temperature and pressure, respectively; and the total mixing ratio of airborne water (water vapor, cloud water and ice)

$$q_t = q_v + q_c + q_i . \qquad (4.2)$$

For the simulation of non-precipitating warm clouds, the three prognostic variables T, q_v and q_c can be replaced equivalently with three other prognostic variables s, q_t and the supersaturation $(q_v/q_{vsw} - 1)$. Of all the other three variables, as shown in Equation (3.6), only the supersaturation involves the short timescale of water vapor condensation. Since cloud condensation (or evaporation) can not change s or q_t, it is reasonable to assume that the supersaturation is zero when cloud water exists[1]. Consequently, three prognostic variables are decreased to two prognostic variables (i.e., s and q_t).

Zero supersaturation implies that air is saturated with respect to water and real supersaturation is removed. In fact, it is impossible for real supersaturation to be simulated in cloud-resolving models even though a small time step is used, because no spectra of cloud particles are represented explicitly.

[1] In spectral-bin models (e.g., Tao *et al.* 2003b), the spectra of cloud particles are represented explicitly. Thus, the approximation of zero supersaturation can be removed and real supersaturation can be simulated properly with a small time step.

Fortunately, the approximation of zero supersaturation is supported by observations. Since real supersaturation in clouds can not be measured directly, it is usually calculated with observational data of temperature, vertical velocity and cloud droplets. It is found that real supersaturation in cumulus clouds is in the range from –0.5 to 0.5% and rarely exceeds 1% (Politovich and Cooper 1988).

The approximation of zero supersaturation is understandable in the atmosphere. When no ice is involved, air containing cloud water is very close to saturation over water because the concentration of cloud condensation nuclei is very high (e.g., Howell 1949; Politovich and Cooper 1988). When ice particles exist, air with cloud water is still close to saturation over water because of the great difference of the concentrations of cloud drops and ice particles (Korolev and Mazin 2003, Zeng, Tao and Simpson 2004). The concentration of cloud drops is about four orders larger than the concentration of ice particles (e.g., Wallace and Hobbs 1977, Pruppacher and Klett 1997). Thus the timescale of cloud water evaporation is much smaller than the timescale of water vapor deposition on ice particles (see Figures 2 and 3 for comparison). As a result, the air with cloud water is almost saturated with respect to water, which provides an environment for the Bergeron process in cold clouds (Bergeron 1935). Summarily, it is physically clear that (s, q_t) can replace (T, q_v, q_c) as prognostic variables in cloud-resolving modeling.

b. Diagnosing temperature from moist entropy

This subsection describes how to diagnose temperature from moist entropy and other prognostic variables. The procedure is summarized in the flow chart in Figure 5. When p

the pressure and q_i the mixing ratio of cloud ice are known, (T, q_v, q_c) the air temperature and the mixing ratios of water vapor and cloud water can be diagnosed from (s, q_t) the moist entropy and the total mixing ratio of airborne water.

Consider an imaginary parcel with s the moist entropy[2], p the pressure and q_i the mixing ratio of cloud ice. The imaginary parcel stays right at water-saturation and contains no cloud water. Its temperature is denoted as T_w^* and its saturation mixing ratio of water vapor as

$$q_{vsw}^* = 0.622 \frac{E_{sw}(T_w^*)}{p - E_{sw}(T_w^*)}. \tag{4.3}$$

Using the preceding equation, Equation (4.1) is solved for T_w^* with the Newton iterative method first. Then, q_{vsw}^* is determined by Equation (4.3).

Since moist entropy and the total mixing ratio of airborne water are conserved when water vapor condensates or cloud drops evaporate, q_{vsw}^* for the imaginary parcel is compared with q_t-q_i for the original parcel, showing whether the original parcel is saturated with respect to water. When q_t-q_i<q_{vsw}^*, the air is unsaturated with respect to water. Thus q_c=0, q_v=q_t-q_i, and Equation (4.1) is solved for the air temperature T with the

[2] When cloud ice is involved, moist entropy changes slightly with temperature in adiabatic motion. Thus, the moist entropy of the imaginary parcel is adjusted to $s + q_i[L_f(T)/T - L_f(T_w^*)/T_w^*]$ so that the imaginary parcel can change adiabatically to the state where moist entropy is the same as that of the original parcel [see Equation (3.5) of Zeng *et al.* (2004) for details]. In other words, $s + q_i L_f(T)/T$ is conserved in cloud condensation (or evaporation).

Newton iterative method. When q_t-$q_i \geq q_{vsw}^*$, the air is saturated with respect to water. As a result, $q_v=q_{vsw}^*$, $T=T_w^*$ and $q_c=q_t-q_v-q_i$.

c. Comparison of two numerical models

In this subsection, two numerical models are used to simulate an air parcel in adiabatic upward motion. They use (T, q_v, q_c) and (s, q_t) as prognostic variables, respectively. Their results are compared to show the benefit of using moist entropy as a prognostic variable.

In the first model, (T, q_v, q_c) are used as prognostic variables. Their governing equations are

$$\frac{dq_c}{dt} = -\frac{dq_v}{dt} \tag{4.4}$$

$$(C_p + C_{pv}q_v + c_l q_c)\frac{dT}{dt} - R_d T \frac{d\ln(p-e)}{dt} - q_v R_v T \frac{d\ln e}{dt} = -L_v \frac{dq_v}{dt} \tag{4.5}$$

$$\frac{dp}{dt} = -\rho g w \tag{4.6}$$

and

$$\frac{dq_v}{dt} = -(1+\frac{q_{vsw}L_v^2}{R_v C_p T^2})^{-1} \frac{q_v - q_{vsw}}{\tau} \tag{4.7}$$

when $q_v > q_{vsw}$. When $q_v < q_{vsw}$, Equation (4.7) still works if $q_c > 0$. Otherwise, $dq_v/dt=0$.

Of the preceding governing equations, Equation (4.6) is obtained from the hydrostatic equation, and Equation (4.7) is obtained from Equations (3.4) and (3.8). As shown in Equation (3.8), the timescale τ changes with time. Its variation can be simulated explicitly in spectral-bin models that explicitly represent the spectrum of cloud drops (e.g., Tao *et al.* 2003b). For simplicity, a constant timescale τ=1 s is used in Equation (4.7) so as to bring the computational phenomena into focus.

In the second model, (s, q_t) are used as prognostic variables. Their governing equations are $ds/dt=dq_t/dt=0$ and Equation (4.6). Both models are equivalent. They involve neither precipitation nor ice. They follow the numerical scheme in Equation (2.2).

The air parcel is assumed to move upward with a vertical velocity of w=4 m/s as well as an initial pressure 1000 hpa, relative humidity of 85% and temperature of 300 K. The numerical results from the two models are displayed in Figure 6. The results from the first model with Δt=0.1 s are displayed with thin solid lines. These results can be regarded as a benchmark to check the results in other cases.

The results from the first model using Δt=3 s are displayed with thin dashed lines in Figure 6. As shown in the figure, the results are bad compared to those with Δt=0.1 s, and both spurious supersaturation and negative mixing ratio of cloud water are present. When the model uses Δt=10 s, it blows up due to computational instability. The results from the second model with Δt=10 s are displayed with thick dashed lines in Figure 6. As shown in the figure, the results agree well with those of the first model with Δt=0.1 s, and neither spurious supersaturation nor negative mixing ratio of cloud water appears. These numerical tests clearly show that moist entropy and the total mixing ratio of airborne water are more efficient than temperature and the mixing ratios of water vapor and cloud water as prognostic variables in cloud-resolving modeling.

5. Summary

Spurious computational phenomena occur in cloud-resolving models when the time step for explicit integration is larger than a microphysical timescale. The phenomena are

evident as spurious supersaturation and negative mixing ratio of cloud water (e.g., Grabowski 1989, Tao *et al.* 1989). The related computational error can affect long-term cloud-resolving modeling significantly (e.g., Robe and Emanuel 1996).

In this paper, the microphysical timescales in clouds are studied in comparison with the time step for cloud-resolving modeling, providing theoretical evidence for the choice of prognostic thermodynamic variables. Of all the microphysical timescales that are analyzed in the paper, only the timescale of water vapor condensation (or cloud water evaporation) is smaller than 10 s, the order of a typical time step used in cloud-resolving modeling, indicating that cloud condensation (or evaporation) is not suitable for explicit simulation in cloud-resolving modeling.

In current cloud-resolving models, the three variables (T, q_v, q_c) are used as prognostic variables to simulate non-precipitating warm clouds. Since all three variables involve the short timescale of water vapor condensation, it is suggested that they be replaced with moist entropy s, the total mixing ratio of airborne water q_t and supersaturation. The supersaturation, rather than s and q_t, involves the short timescale. Therefore, it is reasonable to assume zero supersaturation when cloud water exists, and consequently the three prognostic variables are decreased to two prognostic variables (i.e., s and q_t).

Two numerical models are used to simulate an air parcel in adiabatic upward motion. Their results are compared to show the benefit of using moist entropy as a prognostic variable. The first numerical model uses (T, q_v, q_c) as prognostic variables. When its time step is small (e.g., less than 1 s), its results are reasonable. When its time step is large (e.g., larger than 2 s), its results are overwhelmed with great computational errors, exhibiting the phenomena of spurious supersaturation and negative mixing ratio of cloud

water. The second model uses (s, q_t) as prognostic variables. When its time step is 10 s (or even larger), its results still agree well with those of the first model using a very small time step (e.g., 0.1 s). The comparison of the two models shows clearly that (s, q_t) can work efficiently as prognostic variables in cloud-resolving modeling.

Acknowledgements. The work is supported by the NASA Headquarters Atmospheric Dynamics and Thermodynamics Program and the NASA Tropical Rainfall Measuring Mission (TRMM). The authors are grateful to Dr. R. Kakar at NASA headquarters for his support of this research. The authors also thank Mr. S. Lang for reading the manuscript.

APPENDIX A

List of Symbols

A_w/A_i : defined in (3.3)/(3.10)

$C_p/C_{pv}/c_l$: specific heat of dry air/water vapor/liquid water

D_v : coefficient of water vapor diffusion in air

e : partial pressure of water vapor

E_{sw}/E_{si} : saturation vapor pressure over water/ice

$f=e/E_{sw}$: relative humidity

f_v/f_h : ventilation coefficient for water vapor diffusion/heat transport

g : acceleration due to gravity

K_a : coefficient of air heat conductivity

$L_v/L_s/L_f$: latent heat of vaporization/sublimation/freezing

$N_c/N_r/N_i/N_p$: concentration of cloud droplets/raindrops/cloud ice particles/precipitating ice particles

p : total pressure of moist air

$p_{ref}=10^5$ pa : reference pressure

q_{vsw}/q_{vsi} : saturation mixing ratio of water vapor over water/ice

$q_v/q_c/q_i/q_r/q_s/q_g$: mixing ratio of water vapor/cloud water/cloud ice/rain/snow/graupel

$q_t=q_v+q_c+q_i$: total mixing ratio of airborne water

$r_c/r_r/r_i/r_p$: radius of cloud droplets/raindrops/cloud ice particles/precipitating ice particles

R_d/R_v : gas constant of dry air/water vapor

s : moist entropy per unit mass

t : time

T : temperature

T_o=273.15 K : absolute temperature at the melting point

T_{ref} =273.15 K : reference temperature

w : vertical velocity

z : height

τ: timescale

Δt : time step for integration

ρ : air density

ρ_w/ρ_i : density of liquid water/ice

REFERENCES

Albrecht, B. and S. K. Cox, 1975: The large-scale response of the tropical atmosphere to cloud-modulated infrared heating. *J. Atmos. Sci.*, **32**, 16-24.

Baker, M. B., 1997: Cloud microphysics and climate. *Science*, **276**, 1072-1078.

Bergeron, T., 1935: On the physics of clouds and precipitation. *Proc. 5th Assembly U.G.G.I.*, Lisbon, Portugal, 156-180.

Grabowski, W. W., 1989: Numerical experiments on the dynamics of the cloud-environment interface: small cumulus in a shear-free environment. *J. Atmos. Sci.*, **46**, 3513-3541.

Grabowski, W. W. and P. K. Smolarkiewicz, 1990: Monotone finite-difference approximations to the advection-condensation problem. *Mon. Wea. Rev.*, **118**, 2082-2097.

Howell, W. E., 1949: The growth of cloud drops in uniformly cooled air. *J. Meteor.*, **6**, 134-149.

Korolev, A. V. and I. P. Mazin, 2003: Supersaturation of water vapor in clouds. *J. Atmos. Sci.*, **60**, 2957-2974.

Margolin, L., J. M. Reisner and P. K. Smolarkiewicz, 1997: Application of the volumn-of-fluid method to the advection-condensation problem. *Mon. Wea. Rev.*, **125**, 2265-2273.

Ooyama, K. V., 1990: A thermodynamic foundation for modeling the moist atmosphere. *J. Atmos. Sci.*, **47**, 2580-2593.

Ooyama, K. V., 2001: A dynamic and thermodynamic foundation for modeling the moist atmosphere with parameterized microphysics. *J. Atmos. Sci.*, **58**, 2073-2102.

Politovich, M. K. and W. A. Cooper, 1988: Variability of the supersaturation in cumulus clouds. *J. Atmos. Sci.*, **45**, 1651-1664.

Pruppacher, H. R. and J. D. Klett, 1997: *Microphysics of clouds and precipitation.* Kluwer, 954 pp.

Raymond, D. J., 2000: The Hadley circulation as a radiative-convective instability. *J. Atmos. Sci.*, **57**, 1286-1297.

Raymond, D. J. and A. M. Blyth, 1986: A stochastic mixing model for nonprecipitating cumulus clouds. *J. Atmos. Sci.*, **43**, 2708-2718.

Raymond, D. J. and X. Zeng, 2000: Instability and large-scale circulations in a two-column model of the tropical troposphere. *Quart. J. Roy. Meteor. Soc.*, **126**, 3117-3135.

Riehl, H. and J. S. Malkus, 1958: On the heat balance in the equatorial trough zone. *Geophysica*, **6**, 503-538.

Robe, F. R. and K. A. Emanuel, 1996: Moist convective scaling: some inferences from three-dimensional cloud ensemble simulations. *J. Atmos. Sci.*, **53**, 3265-3275.

Simpson, J., R. F. Adler and G. R. North, 1988: A proposed Tropical Rainfall Measuring Mission (TRMM) satellite. *Bull. Amer. Meteor. Soc.*, **69**, 278-295.

Squires, P., 1952: The growth of cloud drops by condensation. *Aust. J. Sci. Res.*, **5**, 59-86.

Tao, W.-K. and R. Adler, 2003a: Cloud systems, hurricanes, and the Tropical Rainfall Measuring Mission (TRMM) —— A tribute to Dr. Joanne Simpson. *Meteor. Monogr.*, No. 51, Amer. Meteor. Soc., 234pp.

Tao, W.-K., J. Simpson, D. Baker, S. Braun, M.-D. Chou, B. Ferrier, D. Johnson, A. Khain, S. Lang, B. Lynn, C.-L. Shie, D. Starr, C.-H. Sui, Y. Wang and P. Wetzel,

2003b: Microphysics, radiation and surface processes in the Goddard Cumulus Ensemble (GCE) model. *Meteor. Atmos. Phys.*, **82**, 97-137.

Tao, W.-K. and J. Simpson, 1993: The Goddard Cumulus Ensemble model. Part I: Model description. *Terr. Atmos. Oceanic Sci.*, **4**, 19-54.

Tao, W.-K., J. Simpson and M. McCumber, 1989: An ice-water saturation adjustment. *Mon. Wea. Rev.*, **117**, 232-235.

Tompkins A. M. and G. C. Craig, 1998: Radiative-convective equilibrium in a three-dimensional cloud ensemble model. *Quart. J. Roy. Meteor. Soc.*, **124**, 2073-2098.

Wallace, J. M. and P. V. Hobbs, 1977: *Atmospheric Science: An Introductory Survey.* Academic Press, New York, 467pp.

Zeng, X., 2001: *Ensemble simulation of tropical convection.* Ph.D. dissertation, New Mexico Tech. New Mexico Tech Library, 124pp.

Zeng, X., W.-K. Tao and J. Simpson, 2004: An equation for moist entropy in a precipitating and icy atmosphere. Submitted to *J. Atmos. Sci.* (accepted).

Figure Captions

Figure 1 The variable ϕ in the vertical axis varies with time when Δt=10 s and the timescale τ is 2, 5 and 12.5 s, respectively. The numerical and the analytical solutions are shown with thick and thin lines, respectively.

Figure 2 The timescale of water vapor condensation varies with pressure (or temperature). The results with $N_c r_c$= 500 and 3000 $\mu m \cdot cm^{-3}$ are displayed with thin and thick lines, respectively.

Figure 3 The timescale of water vapor deposition varies with pressure (or temperature). The results with $N_i r_i$=10^{-3}, 10^{-1} and 10^{1} $\mu m \cdot cm^{-3}$ are displayed with dashed, thin and thick lines, respectively.

Figure 4 The timescale of ice fusion varies with $N_p r_p$. The timescales for cloud ice fusion and snowflake fusion are displayed with thin and thick lines, respectively.

Figure 5 Schematic on the diagnosis of temperature from moist entropy and the total mixing ratio of airborne water.

Figure 6 Change in output variables with height for two different models. The variables in a traditional model with Δt=0.1 s are displayed with thin solid lines; those in the traditional (or first) model with Δt=3 s are displayed with thin dashed lines; and those in

the present (or second) model with Δt=10 s are displayed with thick dashed lines. Thin solid lines coincide with thick dashed lines.

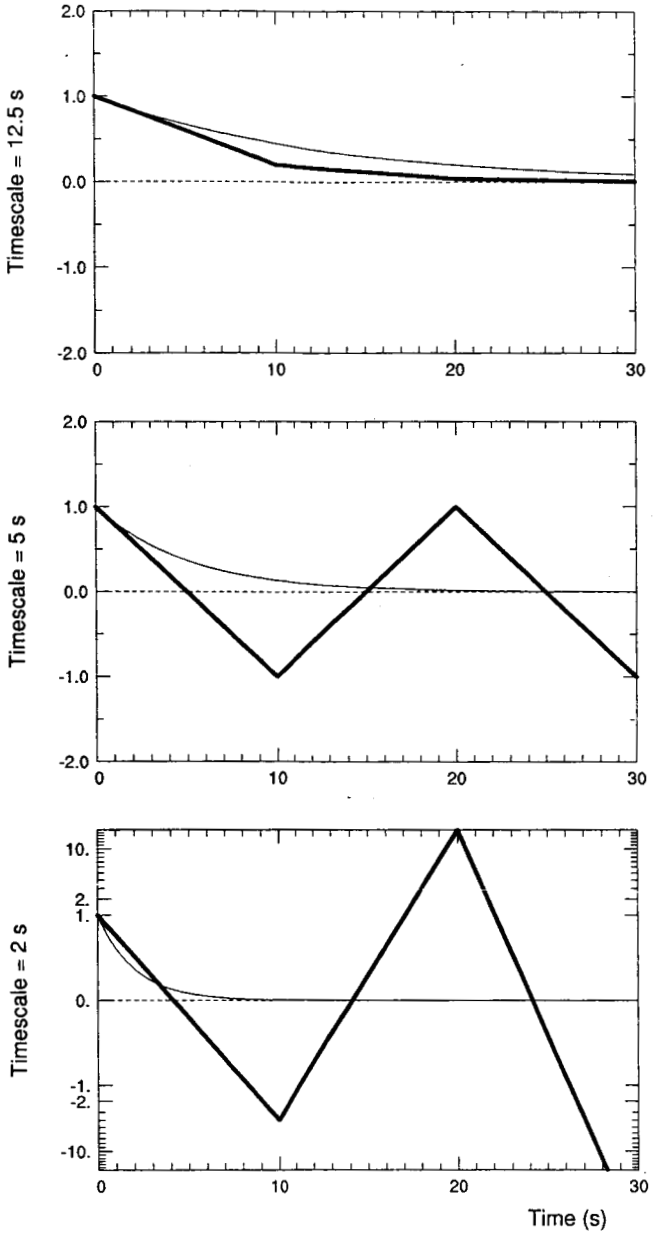

Figure 1 The variable ϕ in the vertical axis varies with time when Δt=10 s and the timescale τ is 2, 5 and 12.5 s, respectively. The numerical and the analytical solutions are shown with thick and thin lines, respectively.

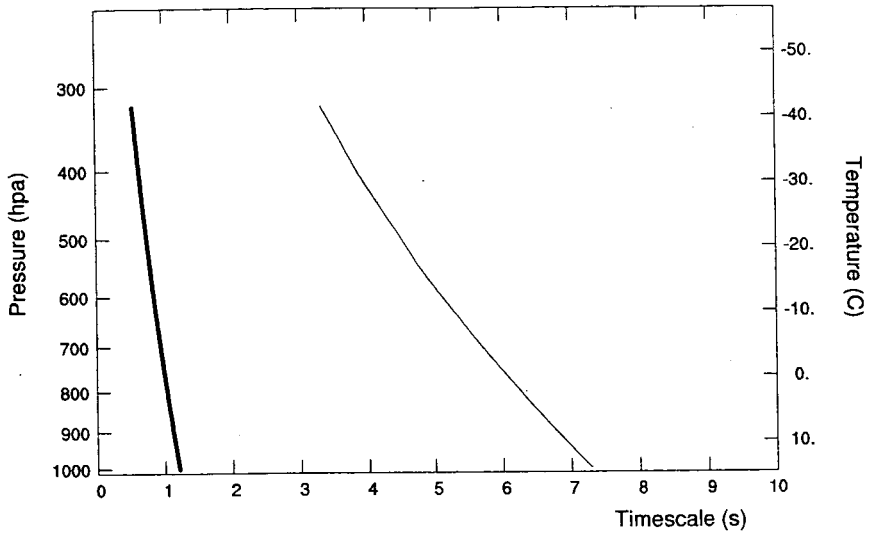

Figure 2 The timescale of water vapor condensation varies with pressure (or temperature). The results with $N_c r_c$= 500 and 3000 μm·cm^{-3} are displayed with thin and thick lines, respectively.

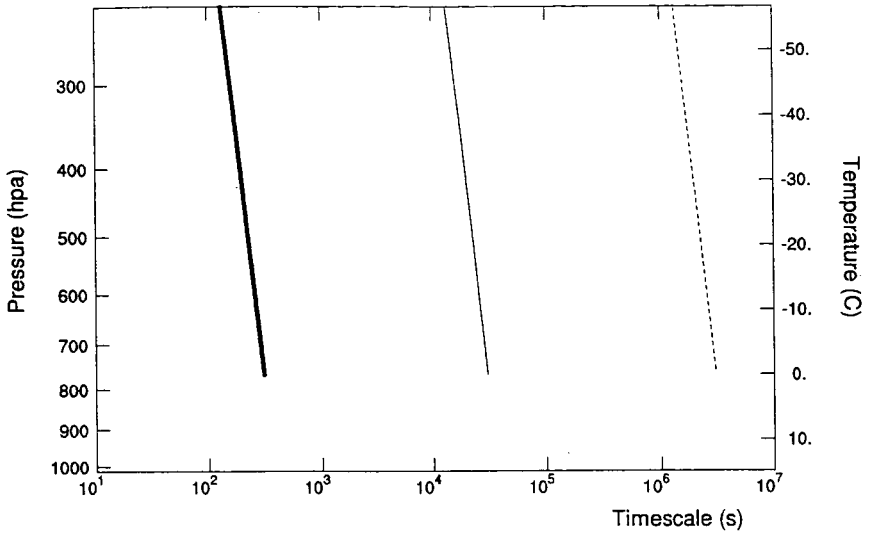

Figure 3 The timescale of water vapor deposition varies with pressure (or temperature). The results with $N_i r_i$=10^{-3}, 10^{-1} and 10^{1} μm·cm^{-3} are displayed with dashed, thin and thick lines, respectively.

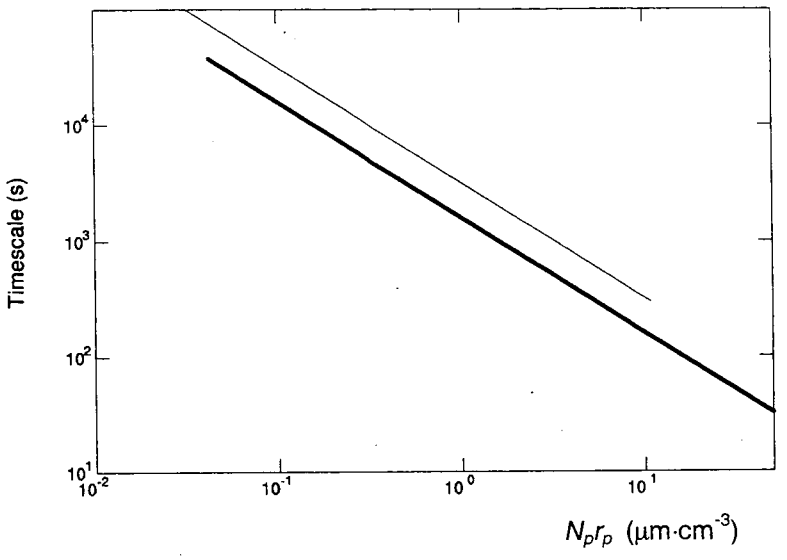

Figure 4 The timescale of ice fusion varies with $N_p r_p$. The timescales for cloud ice fusion and snowflake fusion are displayed with thin and thick lines, respectively.

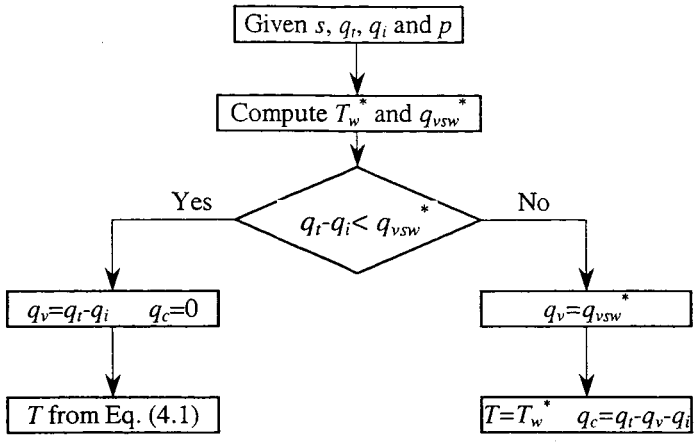

Figure 5 Schematic on the diagnosis of temperature from moist entropy and the total mixing ratio of airborne water.

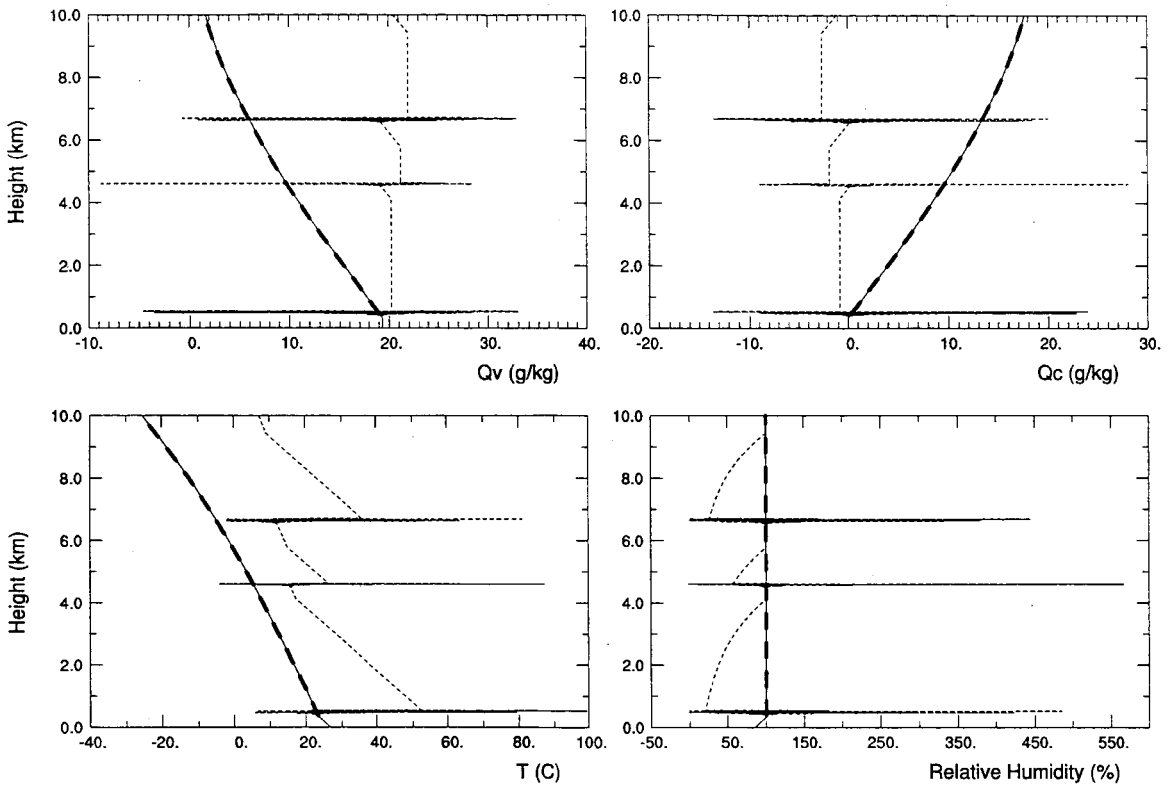

Figure 6 Change in output variables with height for two different models. The variables in a traditional model with Δt=0.1 s are displayed with thin solid lines; those in the traditional (or first) model with Δt=3 s are displayed with thin dashed lines; and those in the present (or second) model with Δt=10 s are displayed with thick dashed lines. Thin solid lines coincide with thick dashed lines.

Microphysical Timescales in Clouds and their Application in Cloud-Resolving Modeling

Xiping Zeng

Goddard Earth Sciences and Technology Center, University of Maryland, Baltimore County, and Laboratory for Atmospheres, NASA Goddard Space Flight Center, Greenbelt, Maryland

Wei-Kuo Tao and **Joanne Simpson**

Laboratory for Atmospheres, NASA Goddard Space Flight Center, Greenbelt, Maryland

Popular Summary

Spurious computational phenomena (e.g., spurious supersaturation and negative mixing ratio of cloud water) exist in current cloud-resolving modeling. They originate in the interaction between model dynamics and cloud microphysics. In this paper, theoretical analysis is given to show that the phenomena appear while the timescale of cloud condensation or evaporation is smaller than the time step used in cloud-resolving models.

To remove the phenomena, it is suggested that moist entropy be used as a prognostic variable and temperature be diagnosed from that and other prognostic variables. Numerical tests show that the spurious computational phenomena, as expected, disappear when moist entropy is used as a prognostic variable.